

Modelling investigation of water partitioning at a semiarid ponderosa pine hillslope

Huade Guan,^{1*} Jirka Simunek,² Brent D. Newman^{3†} and John L. Wilson¹

¹ Department of Earth and Environmental Science, New Mexico Tech, Leroy Place 801, Socorro, NM 87801, USA

² Department of Environmental Sciences, University of California, Riverside, CA 92521, USA

³ Earth and Environmental Sciences Division, MS J495, Los Alamos National Laboratory, Los Alamos, NM 87545 USA

Abstract:

The effects of vegetation root distribution on near-surface water partitioning can be two-fold. On the one hand, the roots facilitate deep percolation by root-induced macropore flow; on the other hand, they reduce the potential for deep percolation by root-water-uptake processes. Whether the roots impede or facilitate deep percolation depends on various conditions, including climate, soil, and vegetation characteristics. This paper examines the effects of root distribution on deep percolation into the underlying permeable bedrock for a given soil profile and climate condition using HYDRUS modelling. The simulations were based on previously field experiments on a semiarid ponderosa pine (*Pinus ponderosa*) hillslope. An equivalent single continuum model for simulating root macropore flow on hillslopes is presented, with root macropore hydraulic parameterization estimated based on observed root distribution. The sensitivity analysis results indicate that the root macropore effect dominates saturated soil water flow in low conductivity soils (K_{matrix} below 10^{-7} m/s), while it is insignificant in soils with a K_{matrix} larger than 10^{-5} m/s, consistent with observations in this and other studies. At the ponderosa pine site, the model with simple root-macropore parameterization reasonably well reproduces soil moisture distribution and some major runoff events. The results indicate that the clay-rich soil layer without root-induced macropores acts as an impeding layer for potential groundwater recharge. This impeding layer results in a bedrock percolation of less than 1% of the annual precipitation. Without this impeding layer, percolation into the underlying permeable bedrock could be as much as 20% of the annual precipitation. This suggests that at a surface with low-permeability soil overlying permeable bedrock, the root penetration depth in the soil is critical condition for whether or not significant percolation occurs. Copyright © 2010 John Wiley & Sons, Ltd.

KEY WORDS hillslope; percolation; root macropore modelling; recharge; semiarid; ponderosa pine; New Mexico; root distribution; macropore flow

Received 24 February 2009; Accepted 4 November 2009

INTRODUCTION

Groundwater recharge is an important factor for long-term water resource management, especially in arid and semiarid regions. Due to the dry climate, thick vadose zones, and vegetation water uptake, groundwater recharge in arid and semiarid basin floors is typically very small (Phillips, 1994; Izbicki *et al.*, 2000; Walvoord *et al.*, 2002; Flint *et al.*, 2004; Walvoord and Phillips, 2004; Scanlon *et al.*, 2005). Although vegetation functions in partitioning shallow subsurface water in two ways: (1) through root-water-uptake reducing or completely eliminating deep percolation (potential recharge), or even causing vertical groundwater discharge where the water table is shallow, and (2) through root-induced macropores facilitating deep percolation, the first mechanism seems to be dominant in arid and semiarid regions (Gee *et al.*, 1994; Stothoff *et al.*, 1999). With increasing

soil wetness, the second mechanism may become more significant. Rasse *et al.* (2000) demonstrate that Alfalfa root-induced macropores increase saturated soil hydraulic conductivity by 57%, and facilitate deep percolation. Whether the roots impede (by root water uptake) or facilitate (by root-induced macropores) deep percolation depends on various conditions including climate, soil, and vegetation characteristics (Newman *et al.*, 2006), particularly the frequency and duration at which macropores are saturated or nearly saturated (Dong *et al.*, 2003).

Because of increased precipitation and reduced potential evapotranspiration in the mountains, the potential for local water yield increases. Under a conventional assumption of impermeable underlying bedrock, this water yield will contribute to lateral surface runoff and/or interflow along the hillslope. Recent experiments at a humid hillslope site challenge the impermeable-bedrock assumption with observations that bedrock percolation can be a predominant hillslope water loss, even for granite (Tromp-van Meerveld *et al.*, 2007). In most situations, bedrock percolation depends on whether, and how quickly, soil moisture can be transmitted from the root zone into the soil-bedrock interface.

Root induced macropores have been recognized to be effective soil–water conduits in hillslopes (Beven and

* Correspondence to: Huade Guan, School of Chemistry, Physics and Earth Sciences, National Centre for Groundwater Research and Training, Flinders University, GPO Box 2100, SA 5001, Australia. E-mail: huade.guan@flinders.edu.au

† Present address: Brent D. Newman, Isotope Hydrology Section, International Atomic Energy Agency, PO Box 100, Wagramer Strasse 5, Vienna, A1400, Austria.

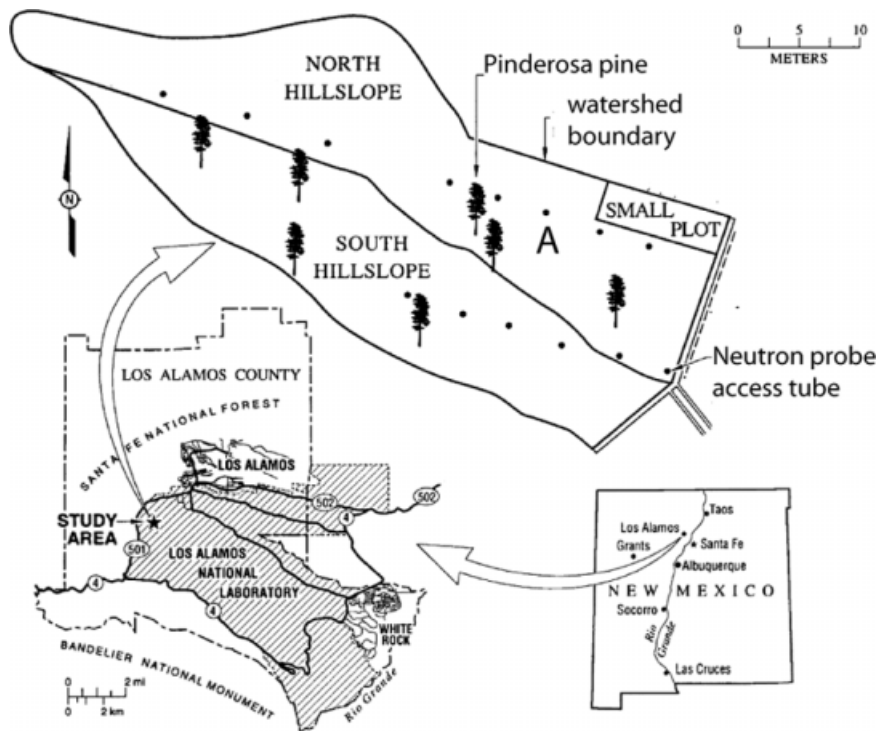


Figure 1. Location map of the study site (adapted from Wilcox *et al.*, 1997)

Germann, 1982; Noguchi *et al.*, 1999). Thus, a deeper root zone can be advantageous for downward water movement into the soil profile. However, a deeper root zone would also amplify root-water-uptake functions, reducing the potential for deep percolation. Thus, the first objective of this paper is to examine how root distribution in a semiarid hillslope affects soil water percolation into the underlying permeable bedrock by numerical modelling.

The study is based on experiments conducted at a ponderosa pine (*Pinus ponderosa*) site in northern central New Mexico, USA. The ponderosa pine site has a low slope (6%), with highly permeable tuff bedrock (saturated hydraulic conductivity, $K_s = 1.8 \times 10^4$ mm/year, or permeability $k = 5.8 \times 10^{-14}$ m²). Field observations suggest only negligible percolation into the bedrock (Wilcox *et al.*, 1997). At this same site, slope-parallel flow through root macropores was observed in a clay-rich soil horizon during the snowmelt seasons (Newman *et al.*, 2004), and during some rain events (Wilcox *et al.*, 1997 and Newman *et al.*, 1998). The sum of surface runoff and interflow through the soil was estimated to be 10–60 mm/year (Wilcox *et al.*, 1997). The rest of the water was returned to the atmosphere through evapotranspiration (ET) (Brandes and Wilcox, 2000). A low-permeability barrier at or above the soil-tuff interface was hypothesized to impede downward movement of water into the highly permeable tuff (Wilcox *et al.*, 1997). However, based on field observations of a transect across the hillslope, Newman *et al.* (2004) suggested that the less permeable soil matrix of the root zone and root-induced macropores together explained the low quantity of bedrock percolation at this site. In contrast to

the conventional notion that the soil is saturated upwards from the soil-bedrock interface during a wetting event, they proposed that at this specific site the soil is saturated from the top of the soil profile by root macropores. Due to the lack of vegetation roots in the soil horizons just above the permeable tuff, wetting to the bedrock rarely happens.

With this in mind, the second objective of this paper is to examine these interpretations regarding low levels of percolation into the highly permeable bedrock at the ponderosa pine hillslope site by investigating water partitioning using numerical simulations. Both root-water-uptake and root-macropore flow processes are considered in these simulations.

THE STUDY SITE AND DATA

The study site is located at an elevation of 2315 m, and covered by sparse ponderosa pine trees with an understory of short grasses (Figure 1). The southeast-facing hillslope has a steepness of about 6%. The soil cover is fairly uniform, about 100 cm thick, with A, Bw, Bt, and CB horizons (Wilcox *et al.*, 1997). Roots occur primarily in the top 70 cm of the soil in the A, Bw, and Bt horizons (Newman *et al.*, 2004). The estimated soil hydraulic properties from soil core measurements are given in Table I (columns 2 through 6). Micrometeorological data were measured at 15-min intervals, with instruments installed at a height of about 2 m above the ground. The data included precipitation, solar radiation, wind speed, relative humidity, and temperature. Precipitation was measured at 1 min intervals. Surface runoff and interflow were monitored on-site every 15 min, and measured at a

Table I. van Genuchten (1980) model parameters and saturated hydraulic conductivities of the four soil horizons and the underlying bedrock

Horizon	α^a (1/cm)	n^a	θ_s^a	θ_r^a	K_{matrix}^c (m/s)	K_{s-x}^d (m/s)	K_{s-z}^e (m/s)
A	0.015	1.33	0.44	0.06	7.5×10^{-7}	9.4×10^{-6}	3.1×10^{-6}
Bw	0.017	1.14	0.39	0.06	5.7×10^{-9}	8.7×10^{-6}	2.3×10^{-6}
Bt	0.0045	1.15	0.44 ^b	0.08	4.0×10^{-9}	9.4×10^{-6}	2.5×10^{-6}
CB	0.016	1.11	0.47	0.06	3.0×10^{-9}	3.5×10^{-9}	3.2×10^{-9}
R (tuff)	0.0014	1.42	0.28	0	5.8×10^{-7}	5.8×10^{-7}	5.8×10^{-7}

^a The van Genuchten model parameters.

^b The saturated volumetric water content was changed from the lab-measured value of 0.4–0.44 to match the observed saturated soil water content in the field.

^c The lab-measured saturated hydraulic conductivity of the soils at various depths, and bedrock near the study site.

^{d,e} The bulk soil saturated hydraulic conductivity in the direction parallel^d and perpendicular^e to the slope surface. The root perimeter aperture was assumed to be 2.7% of the root diameter and the equivalent root dip angle to be 15° from the surface (calibrated based on surface runoff).

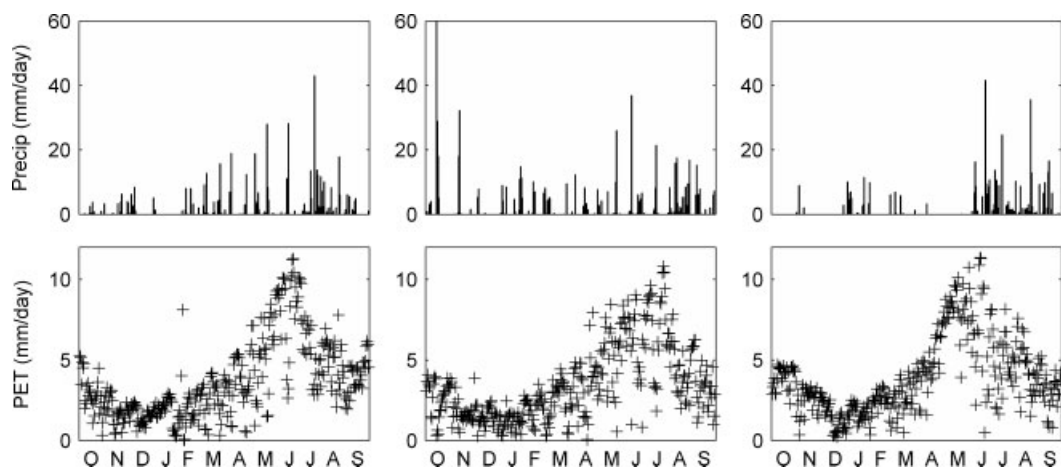


Figure 2. The atmospheric boundary condition for three water years: 1994 (left), 1995 (middle), and 1996 (right) at the ponderosa pine site. The months are listed along the horizontal axis. Only daily data are presented here. The temporal resolution of the data, which was used in HYDRUS simulations, is every 15 min for 1994 and 1995, and every 60 min for 1996. Precipitation is presented here as the sum of rain and snowmelt

1 min interval when there was flow. Soil moisture was measured a few tens of times at various locations and depths during each year.

The atmospheric boundary condition was generated for the numerical simulations described in the next section. The precipitation (P) data (heated gauge data) were used to generate a time-series of water (rainfall + snowmelt) readily available for infiltration and runoff. The total precipitation from October 1993 through August 1998 was 2590 mm, with an annual mean of 527 mm. The recorded precipitation was classified into rainfall and snowfall based on the mean daily temperature (Wigmosta *et al.*, 1994). In this study, we used 0°C for the rainfall and snowfall separation. The snowmelt was estimated using an empirical temperature-index model, in which the snowmelt is linearly related to the daily temperature above a certain threshold (0°C was used). The potential evapotranspiration (PET) was calculated using the Penman-Monteith equation for a hypothetical reference grass using the collected data of solar radiation, temperature, and relative humidity. Since wind speed was not measured above the ponderosa trees, a mean value of 2 m/s was used (Allen *et al.*, 1998). The potential ET during the night (8 pm to 6 am) was assumed to

be zero. The estimated total PET from October 1993 through August 1998 was 6486 mm, with an annual mean of 1319 mm, about 2.5 times the precipitation during this period. Data of three water years (1994–1996, each from the previous October through September) are shown in Figure 2. The seasonality of PET was similar from year to year, while rainfall and snowmelt varied between years. The ratios of PET/P were 2.5, 2, and 3 for 1994, 1995, and 1996 water years, respectively.

NUMERICAL SIMULATIONS

Since root macropore flow was observed (Newman *et al.*, 2004), and ET represents a dominant water balance component at this study site, both are important processes, and need to be considered in the simulations. Various computer codes with differing conceptual models of fracture flows of various complexity (Altman *et al.*, 1996; Simunek *et al.*, 2003), can be used to simulate root-macropore flows. However, since dynamic variations in ET also have to be considered, the choice of computer codes becomes rather limited. HYDRUS is one of a few models that considers both ET and macropore flow processes simultaneously. In order to examine root

macropore flow in two directions (parallel and orthogonal to the slope surface), a two-dimensional version of HYDRUS, called HYDRUS-2D, is used in this study. In HYDRUS, variably saturated water flow in porous media is described using the Richards equation. Evaporation is modelled using a Darcy's law-based extraction function, and transpiration is calculated as a root-distribution-weighted sink term, depending on root-zone soil-water potential and potential transpiration. With its capacity to dynamically relate near-surface water partitioning processes (including evaporation, transpiration, soil water flow) to soil hydraulic properties, root distribution, and the root-water-uptake function, HYDRUS allows us to examine soil and vegetation effects on water partitioning at the hillslope site.

Root macropore modelling

It is challenging to represent the hydrological effects of roots on soil water flow. The difficulties include (1) how to represent the quantitative contribution of an individual root to an increase in the bulk soil hydraulic conductivity, (2) how this contribution varies with soil water potential, (3) how this contribution varies with the direction (e.g. parallel vs. orthogonal to the slope), and (4) how the bulk root-induced hydraulic conductivity is quantitatively related to the observed root distribution. Dong *et al.* (2003) estimated macropore contribution to the bulk soil hydraulic conductivity based on bulk soil water potential and macropore size distribution, which addresses issue (2) quite well. It was developed for one-dimension vertical flow, and not appropriate for simulating water movement on hillslope. In spite of the above challenges, when the boundary conditions and a flow field are known, it is less difficult to estimate macropore equivalent hydraulic properties, which can be defined as those properties subjected to the boundary conditions (Renard and deMarsily, 1997). We will apply the equivalent-property approach to quantify the root macropore effects on the studied hillslope. A similar approach has been used to model subsurface tile-drained soils (Carlier *et al.*, 2007), where equivalent hydraulic conductivity is calculated with drainage density and drain radius.

The procedure to estimate the equivalent anisotropic hydraulic conductivities of a soil with root macropores on a sloping surface, which is related to the observed root distribution, is based on several assumptions. First, that the root macropore contribution to the saturated hydraulic conductivity is quantitatively related to root distribution (e.g. root size and density). Second, that the anisotropy of saturated root macropore flow is quantitatively related to an average root dip angle. Third, that the bulk hydraulic conductivity at various saturations is evaluated using the Mualem (1976) pore size distribution model and the retention properties of the soil matrix. Using a single equivalent porous medium for both macropore and matrix flow leads to a conceptual flaw in that the macropore flow does not cease, as it should, when the

macropore water is drained below a certain degree, but is only reduced by a factor that is related to soil matrix properties. On the other hand, for the same reason, the single equivalent continuum model allows for macropore flow to occur before the soil matrix gets fully saturated, which was commonly observed at the field site (Newman *et al.*, 1998, 2004). Numerically, the single continuum model should work appropriately in simulating water flow at saturated and near-saturated conditions, when the macropore flow is most important.

To formulate the equivalent single continuum model, an individual root macropore is considered as an annular void around the root, with its aperture proportional to the root size (Figure 3). Following Pnueli and Gutfinger (1992), the saturated hydraulic conductivity ($\text{m}\cdot\text{s}^{-1}$) in the longitudinal direction of the slope due to one root, i , parallel with the slope is

$$K_i = \frac{\cos^2 \theta}{A_i \tau} \frac{\rho g \pi (D_i + 2b_i)^4}{128 \mu} C_i \quad (1)$$

and

$$C_i = \left[1 - \left(\frac{D_i}{D_i + 2b_i} \right)^4 - \frac{[1 - (D_i/(D_i + 2b_i))^2]^2}{\ln((D_i + 2b_i)/D_i)} \right] \quad (2)$$

where θ (radian) is the angle between the root and the longitudinal slope direction x (Figure 3), τ (dimensionless) is the tortuosity of the root, which is defined as the ratio of the actual root length over the linear length, D_i (m), b_i (m), and A_i (m^2) are the root diameter, the aperture width, and the cross-sectional area (including aperture) of the root, and ρ ($\text{kg}\cdot\text{m}^{-3}$), g ($\text{m}\cdot\text{s}^{-2}$), and μ ($\text{Pa}\cdot\text{s}$) are the density of liquid water, gravitational acceleration, and the dynamic viscosity of water, respectively.

For a given layer with an isotropic root distribution in the plane parallel to the slope surface, the root-induced saturated hydraulic conductivity is an summation of (1) over different angles θ (from $-\pi/2$ to $\pi/2$) for all different root sizes:

$$K_{\text{root}} = \frac{\rho g \pi}{256 \mu \tau} \frac{\sum_{\text{root-class-}j} [C_j (D_j + 2b_j)^4 n_j]}{\sum_{\text{root-class-}j} [(1/4) \pi n_j (D_j + 2b_j)^2]} \quad (3)$$

where n_j is the number of roots in one root class j with a mean root diameter of D_j observed in the transect, C_j is defined in Equation (2). Equation (3) gives the saturated hydraulic conductivity in the longitudinal direction (x) of the slope due to root macropores, assuming that all roots are in planes parallel to the slope surface.

However, the roots may intercept the slope at a certain angle rather than being parallel to the slope (Figure 3). An equivalent root dip angle is used to lump all roots. In areas with similar surface vegetation coverage and soil water conditions, the equivalent root dip angles should be similar. In this situation, root macropores also contribute to water flow in the z direction, where z is the downward direction orthogonal to x . A contribution

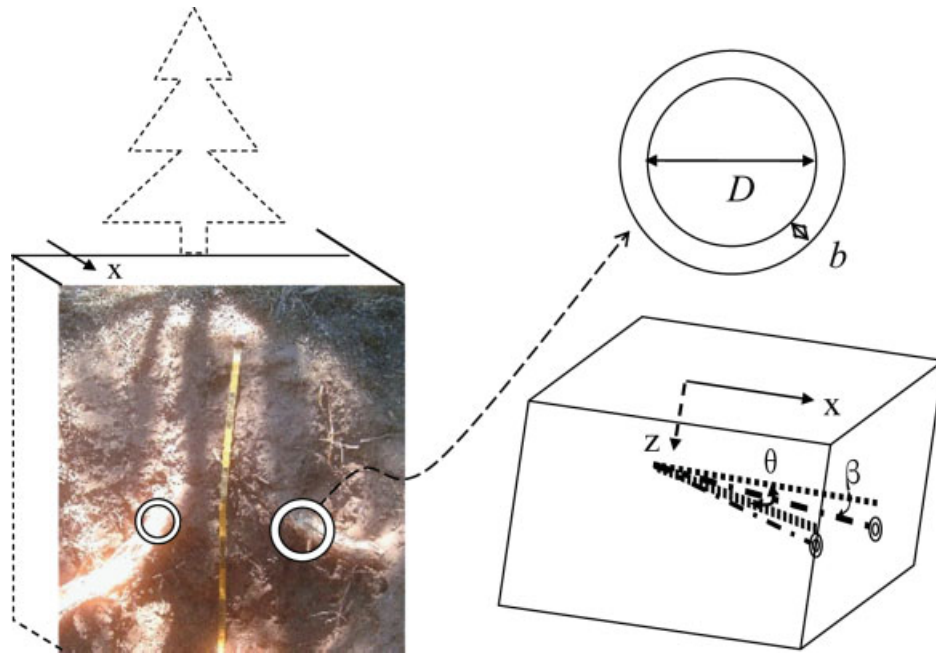


Figure 3. Conceptualization of the hydraulic effects of root macropores, where D is the root diameter, b is the annular void between the root surface and surrounding soil matrix, x is the longitudinal direction parallel to the slope surface, and z is the downward direction perpendicular to x , β is average root dip angle, and θ is the angle between individual root projection on the slope surface and the x direction

of root macropores to the hydraulic conductivity in the z direction is as follows:

$$K_{z_{root}} = \frac{\rho g \pi \sin \beta}{256 \mu \tau} \frac{\sum [C_j (D_j + 2b_j)^4 n_j]}{\sum [(1/4) \pi n_j (D_j + 2b_j)^2]} \quad (4)$$

where β (radian) is the equivalent root dip angle with respect to the slope surface. The saturated hydraulic conductivity in the x direction has to be modified as well, resulting in

$$K_{x_{root}} = \frac{\rho g \pi \cos \beta}{256 \mu \tau} \frac{\sum [C_j (D_j + 2b_j)^4 n_j]}{\sum [(1/4) \pi n_j (D_j + 2b_j)^2]} \quad (5)$$

The bulk saturated hydraulic conductivities ($m \cdot s^{-1}$) in x and z directions are then given by

$$K_{z_{bulk}} = K_{z_{root}} n_{root} + K_{matrix} (1 - n_{root}) \quad (6)$$

and

$$K_{x_{bulk}} = K_{x_{root}} n_{root} + K_{matrix} (1 - n_{root}) \quad (7)$$

where n_{root} is the volumetric fraction occupied by the roots and their surrounding voids, defined as

$$n_{root} = \sum_{j=1}^{size_class} \left[\rho_r^j \frac{\pi}{4} (D_j + 2b_j)^2 \right] \quad (8)$$

where ρ_r^j (m^{-2}) is the root density of the root-size class j and K_{matrix} the soil matrix saturated hydraulic conductivity. The root density (ρ_r) is measured in transects orthogonal to the sloping direction and reported as a number of roots per unit area for each root-size class.

Evaporation and transpiration modelling

It is estimated that over 90% of soil water loss at the study site was due to ET (Brandes and Wilcox, 2000). It is therefore important to appropriately represent evaporation and transpiration processes in order to simulate soil water partitioning correctly. Evaporation and transpiration processes were modelled separately, according to the surface vegetation coverage. Potential evaporation (PE) and potential transpiration (PT) are input to the model, defining the maximum rate of simulated evaporation and transpiration. In HYDRUS, evaporation is calculated from PE dependent of the surface soil moisture availability. A critical water potential is prescribed to determine the threshold above which evaporation occurs at the rate of PE. When the surface soil water potential is below (drier than) this critical value, the boundary condition is set equal to this critical water potential and the actual evaporation is determined by how quickly the soil moisture moves toward the surface according to Darcy's law. Apparently, simulated evaporation is sensitive to the prescribed critical value. According to Rassam *et al.* (2003), for silty soils in the study area, a value of -1000 m was applied.

In HYDRUS, transpiration is calculated from PT multiplied by a scaling function dependent of root-zone soil moisture availability. An S-shape root-water-uptake function (the scaling function) (van Genuchten, 1987) was used

$$\alpha = \frac{1}{1 + (h/h_{50})^p} \quad (9)$$

where α (dimensionless) is the ratio of the actual root-water-uptake rate to its potential rate, in which the potential rate is determined from PT and root distribution function, h (m) the soil water potentials, h_{50} (m) the

soil water potential at which α is reduced by 50%, and p (dimensionless) an experimental constant. A wilting-point soil water potential, below which α is set to zero, is prescribed to mimic the termination of transpiration due to extreme soil moisture stress.

Separated PE and PT inputs are required for evaporation and transpiration modelling. Partitioning of PET into potential evaporation (PE = 70% PET) and potential transpiration (PT = 30% PET) was roughly estimated based on the fractional surface coverage of the ponderosa pine trees at the study site. In addition to the ponderosa pine, sub-story grass also contributes to transpiration. However, since the rooting depth of grass is relatively shallow when compared to pine roots, grass transpiration can be technically mimicked using evaporation. The root density was calculated according to Newman *et al.* (2004), with the A and Bw horizons containing about 65% of roots and the Bt horizon the remaining 35%.

Numerical set-up

The simulations were based on data at location A on the north hillslope (Figure 1). A two-dimension hillslope section (Figure 4), 1 m wide and 2 m deep, was used for the numerical simulations. The soil profile consisted of four soil horizons (A: 10 cm, Bw: 20 cm, Bt: 40 cm, and CB: 30 cm thick) according to Wilcox *et al.* (1997) and had a root zone in the top three soil horizons (Newman *et al.*, 2004). The soil hydraulic properties (Table I) and root distribution were assumed to be homogeneous in each soil horizon. A prescribed constant gradient, $0.5 \sin(2\gamma)$, where γ (radian) is the slope angle, was assigned to each side of the soil profile, mimicking a continuous hillslope condition. Runoff was modelled as an infiltration-excess process consistent with the field results of Wilcox *et al.* (1997), without considering downslope propagation. An atmospheric boundary condition with an interval of 15–60 min was prescribed at the top end of the flow domain, while a free drainage boundary condition was applied at the bottom of the domain (Figure 4).

The parameterization of the S-shape root-water-uptake model was manually adjusted to fit the measured soil water contents. Since root macropores strongly influence the soil infiltration capacity, simulations with bulk soil hydraulic conductivities considering root-macropore effects were tested against the observed runoff, to find the appropriate parameterization of the root macropore model.

RESULTS AND DISCUSSION

Sensitivity analysis of the root macropore model and simulation results

A sensitivity analysis of the root macropore model was conducted against the matrix hydraulic conductivity, the size of the root-macropore aperture, and the root dip angle (Figure 5). The relative contribution of root macropores to the bulk hydraulic conductivity is related to soil and root density, size, and direction. To examine

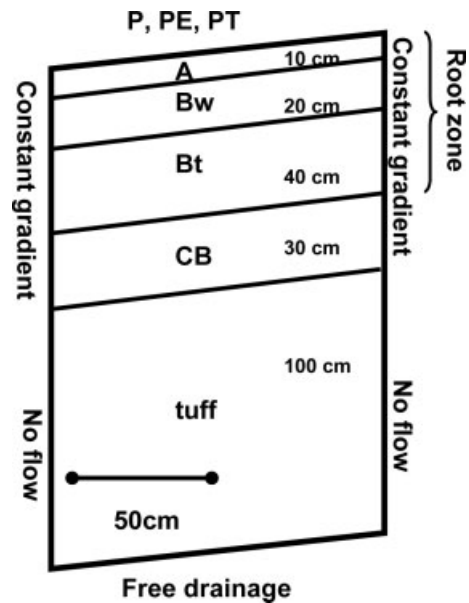


Figure 4. A schematic graph showing the two-dimension, 1-m-wide hillslope section used for the simulations

the effect of the soil matrix, we used the root distribution observed in the A-horizon, a root dip angle of 15° , and an aperture of 2.7% root diameter (this value is estimated from calibration as described in the next paragraph). The results show that the contribution of root macropores dominates the bulk soil hydraulic conductivity when K_{matrix} is smaller than 1×10^{-7} m/s, while it becomes insignificant when K_{matrix} is larger than 1×10^{-5} m/s (Figure 5a). The actual K_{matrix} of the A-horizon is 7.5×10^{-7} m/s (Table I), indicating that both the soil matrix and root macropores are important for infiltration at the study site. Parameterization of the root macropore model should thus be sensitive to the infiltration-excess runoff. The bulk hydraulic conductivity in the z direction (Figure 3) was calculated using the laboratory-measured soil hydraulic properties and observed root density for various root-macropore apertures (Figure 5b) and dip angles (Figure 5c). The bulk hydraulic conductivity of the CB horizon was not sensitive to root parameters, because only a few roots were present at this depth. On the other hand, the bulk hydraulic conductivity for the top three horizons was sensitive to both root factors.

Consequently, calibration of root parameters (dip angle and aperture) against the observed runoff did not provide a unique solution. To overcome the problem of non-uniqueness, a root dip angle of 15° was fixed and only the root aperture was optimized. An angle of 15° should be close to the actual root distribution in the near-surface, where horizontal roots are dominant. Although different root dip angles could be used at different depths, only one root dip angle was used in the simulations, due to the difficulty with the calibration process. This may slightly affect the simulated values of interflow and percolation. Root-macropore aperture is assumed to be proportional to root diameter. Several different aperture sizes were applied for the simulations for the 1994 water year. The one of 2.7% root diameter,

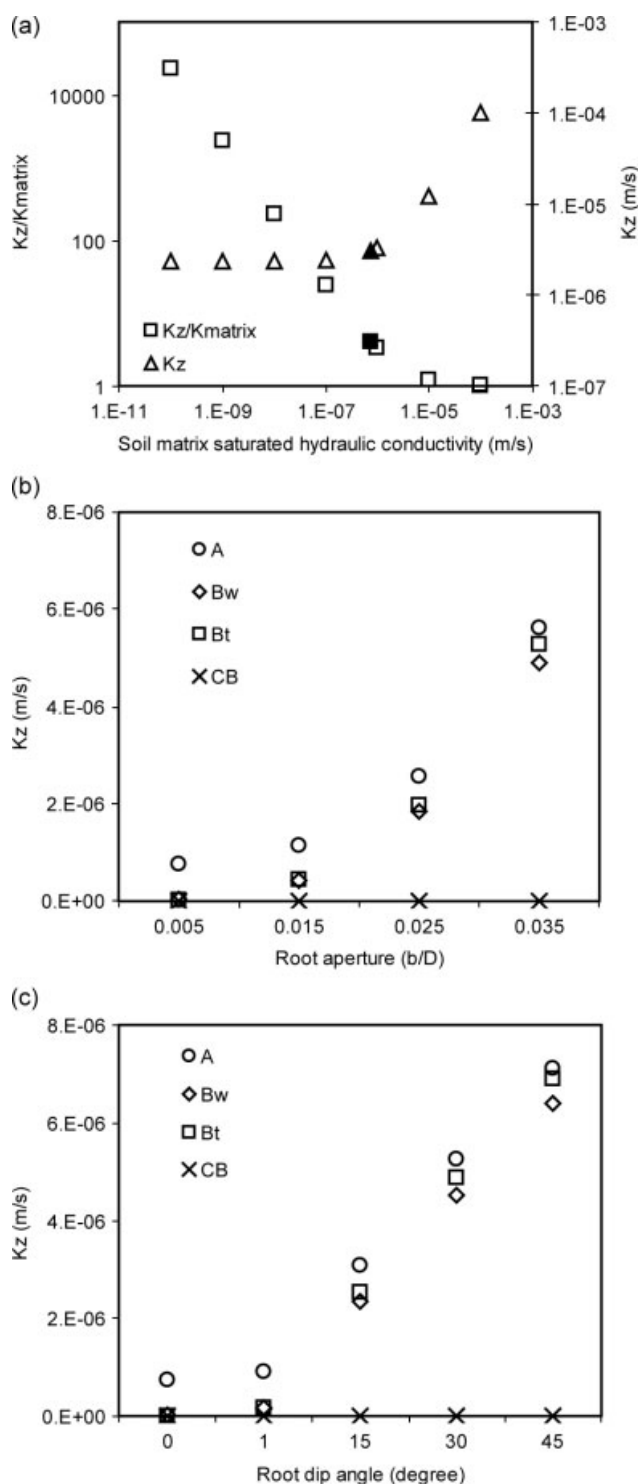


Figure 5. Sensitivity analysis of the root macropore model. (a) The saturated hydraulic conductivity (K_z) perpendicular to the slope surface as a function of the soil matrix hydraulic conductivity. K_z was calculated using the root distribution data observed in the A horizon. The two solid symbols represent the measured A-horizon matrix hydraulic conductivities. (b) K_z calculated as a function of the root-macropore aperture, which is defined as the ratio between b and D (Figure 3), for an equivalent root dip angle of 15° . (c) K_z calculated as a function of the root dip angle for the root aperture of 0.027

which best fits the observed runoff, was chosen. The simulation reproduces two of the three major infiltration-excess runoff events observed on the north hillslope,

but misses the first one in the year (Figure 6). Similar simulations, without considering root macropore effects, were performed, with the result of a modelled runoff over four times of the observation in the 1994 water year (not shown). With the root-induced macropore effects considered, the modelled runoff is about the same amount of the observation. The difference between the modelled and observed first runoff event could be due to either modelling failure or the heterogeneity effect in rainfall and runoff generation between the small catchment and the simulated location. One common problem leading to failure in runoff simulations could be resulted from a low temporal-resolution precipitation input. Because precipitation was input at 15-min resolution, this problem is less likely. Other factors, such as rainfall size, and dry interval, do not explain the apparent modelling failure either, because similar situations occurs either in runoff event (2) or (3).

After calibration with the 1994 water year data, simulated volumetric water content fairly well matched the observations in all 3 years (Figure 7). The abrupt change in the modelled volumetric soil water content at 1 m depth is due to the prescribed material change from the soil to the tuff. Although the soil thickness was observed about 1 m thick, it varies slightly from one location to another. Moreover, the soil-tuff interface is not flat and abrupt. Some surface relief and/or weathering could lead to a soil-moisture transition zone between the soil and underlying tuff. Thus, it is appropriate to compare modelled volumetric moisture content below 1 m depth to the observed moisture content below the transition zone (Figure 7). Big deviation between the modelling results and observations in the 180th day of 1995 water year are probably related to a recent focused snowmelt event, which was not included in the simulation. In preparing the atmospheric boundary conditions, snow was assumed to be uniformly distributed on the surface. In reality, snow might have piled locally, and melt to feed a small area of the catchment. If this happened near location A (Figure 1) some time before the 180th day, it might saturate the soil. The saturated soil in depth could persist to the 180th day of the water year (Figure 7). This possibility is supported by over 0.45 volumetric water content, almost at saturation, in comparison to 0.4 in the other days.

Root-water-uptake model calibration and soil moisture partitioning

The root-water-uptake model was calibrated against the root-zone soil moisture for the 1994 water year (Figure 7). The wilting point water potential was prescribed to be -250 m, close to the observed root vulnerability curve (percentage loss of xylem conductivity vs. water potential) (Stout and Sala, 2003). The calibration process produced h_{50} of -5 m and p of 2 (Equation 9), however, this is quite different from the reported vulnerability curve (Stout and Sala, 2003). If we assume that the root vulnerability curve can be used for root-water-uptake model, the fitted value of h_{50} for the ponderosa pine

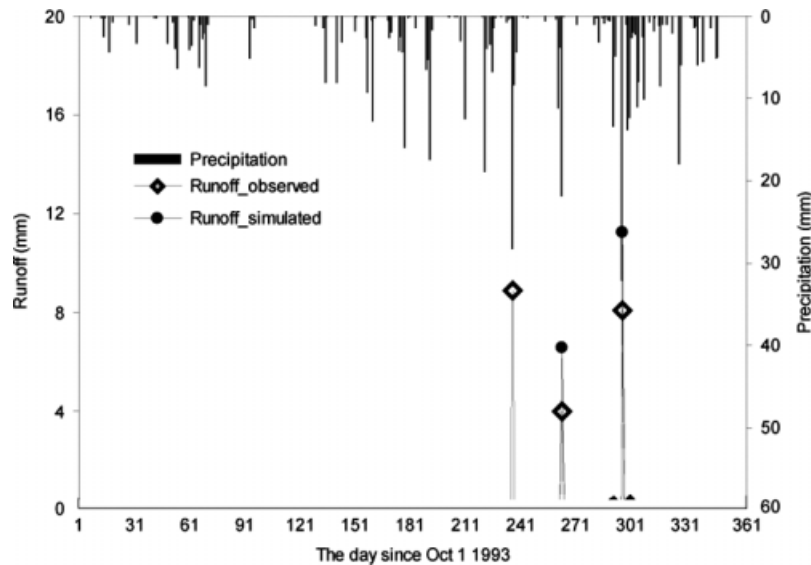


Figure 6. Observed and simulated major daily runoff events in the 1994 water year (Oct 1, 1993—Sept 30, 1994). Daily precipitation (rain + snowmelt) time series are shown for comparison

would be -80 m and of p equal to 2.7. Using this parameterization, simulated root-zone soil moisture is much drier than that observed. A few reasons may explain the inconsistency between the calibrated h_{50} and that determined from the measured root vulnerability curve. First, the transpiration process is affected by the hydraulic conductivity of the root, stem, and leaf conductance. As the vulnerability curve represents only the response of root and/or stem to the moisture stress, it does not include the vegetation regulation of transpiration by leaf stomata. Thus, the parameterization obtained from the vulnerability curve represents only the lower bound for h_{50} . When leaf regulation is also considered, h_{50} may occur in much wetter conditions. Second, as the effect of osmotic potential was not considered in the simulation, h_{50} calibrated against the observed soil moisture can represent slightly wetter conditions than the actual soil water potential, which includes both the matrix and osmotic potentials. Third, as the two parameters (h_{50} and p) were calibrated simultaneously, the results could be nonunique and deviate from the real values. However, the latter two effects generally do not play a big role. Therefore, the first effect is likely the main reason for the difference between the two sets of obtained root water uptake parameters. This indicates that the root (or stem) xylem vulnerability curve is probably not appropriate for parameterizing root-water-uptake models.

The 1994 water year had an annual precipitation close to average long-term conditions. The initial condition for the 1994 water-year simulation was obtained by rerunning the same 1994 climate forcing several times to achieve a quasi-steady state. With root-macropore and ET models calibrated against observations from the 1994 water year, additional simulations were conducted to examine the soil water partitioning for the 1995 and 1996 water years (Figure 7 and Table II). Initial conditions for the 1995 and 1996 water years were based on simulations of the previous water years. The root

mean square errors of the simulated soil moisture at 5 depths for 20 observation times are 0.09, 0.08, and 0.07, in comparison to mean observed soil moisture of 0.30, 0.35, and 0.28, respectively, for the three water years. While annual percolation into the tuff at the ponderosa site was simulated to be less than 5 mm (or 1% of precipitation), simulated evapotranspiration accounted for 94% of annual precipitation in 1994 (Table II, column #2). Percolation into the tuff in both 1995 and 1996 was similar to that of the 1994 water year, i.e. less than 1% of annual precipitation (Table II, columns #2 ~ 4). From these simulations, it appears that groundwater recharge (percolation) at this location is not significant, which is consistent with the previous study of this site (Wilcox *et al.*, 1997). The modelled average ET for the 3-year period is 95% of the total precipitation, which is in agreement with previous water balance analyses of the field data (Brandes and Wilcox, 2000). Simulated interflow during the 3 years is of trace amount, similar to what was observed (Wilcox *et al.*, 1997).

The effects of impeding layer and root macropore on groundwater recharge

Wilcox *et al.* (1997) suggested that an impeding layer of low permeability may restrict downward water movement into the bedrock at the ponderosa pine site. At this site, an abrupt change in soil matrix permeability occurs at a depth of about 10 ~ 20 cm in the Bw horizon (Table I). However, soil water in the field was observed to pond at a depth of 70 cm, around the interface between the Bt and CB horizons. Apparently, the soil hydraulic conductivity of the matrix cannot explain a hypothetical impeding layer at this site. Wilcox *et al.* (1997) hypothesized three potential impeding layers: (1) CB horizon, (2) the base of the Bt horizon, and (3) a thin 'smear' of translocated clay at the soil-tuff interface. Newman *et al.* (2004) suggested that the absence of root macropores at

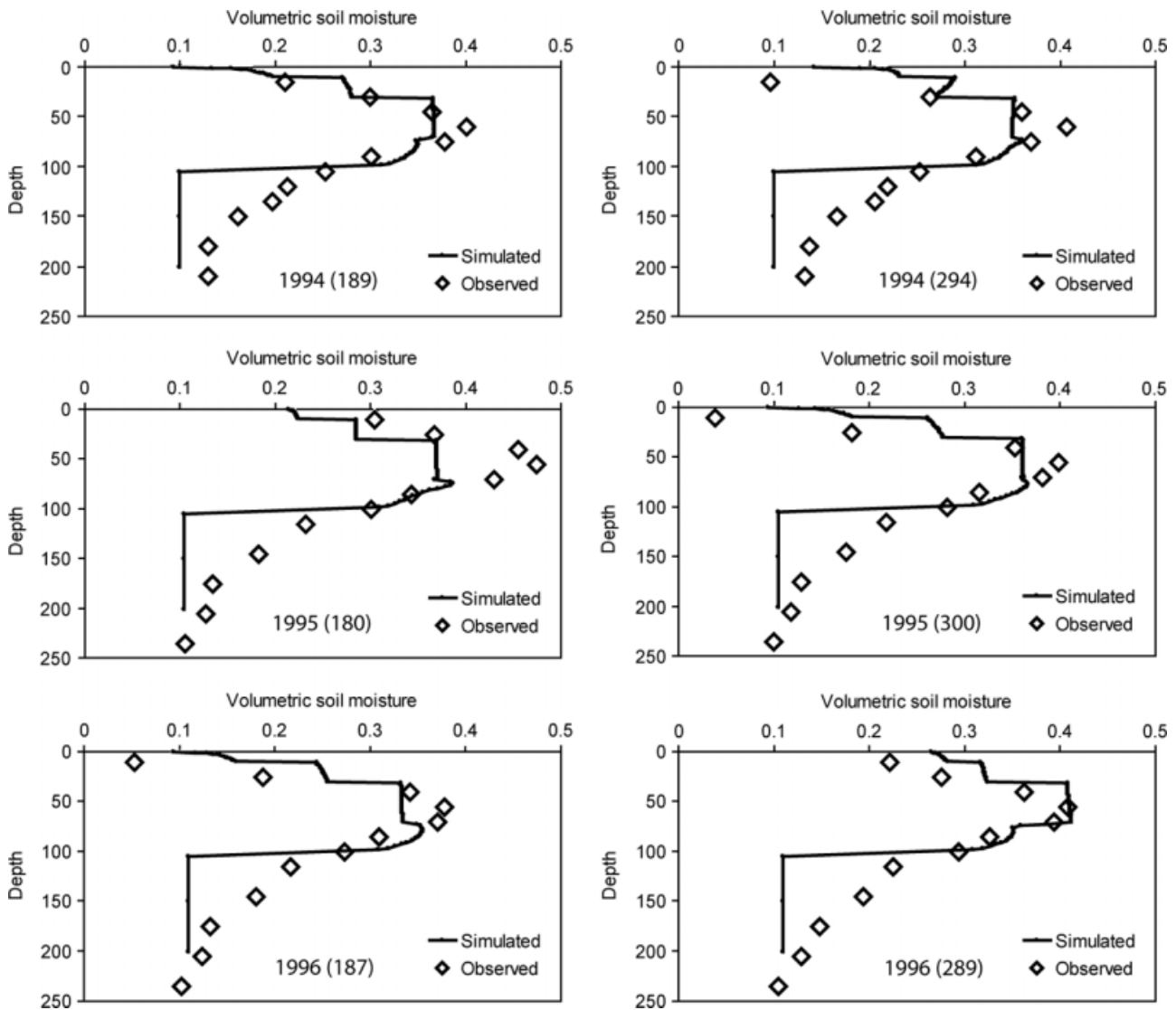


Figure 7. Simulated (lines) and observed (open diamonds) soil water contents (dimensionless) versus the depth (cm) at selected days (the number is given in each panel) for three water years. Selected days are either following the snowmelt season or in the summer monsoon season. Big deviations between modelling results and observations in 1995(180) are probably due to a recent focused snowmelt near location A, which was not represented in the simulations

Table II. Simulated water fluxes (in equivalent depths of mm/year) for the hillslope

Water year	Observed soil profile			Hypothetical soil profile ^a
	1994	1995	1996	
Precipitation (P)	524	686	467	524
Infiltration	506	637	467	506
ET	490	598	435	379
Runoff	18	49	0	18
Percolation	<5	<5	<5	108
ET/P	93%	87%	93%	72%
Percolation/P	<1%	<1%	<1%	21%

^a It was assumed that the root zone directly contacts the underlying tuff by replacing the CB horizon with tuff.

depths below 70 cm could explain an impeding layer at this depth.

Because of modifications due to root-induced macropores, the clay-rich soil of the root zone has a vertical

bulk saturated hydraulic conductivity close to that of the loam soil (Table I). With fewer roots in the CB horizon (or the bottom of the Bt horizon), the soil hydraulic conductivity is about three orders of magnitude lower. The root-induced macropore modification of the bulk saturated hydraulic conductivity of this clay-rich soil (by a factor of 10^3) is much larger than the enhancement factor of 1.5 found by Rasse *et al.* (2000) at an alfalfa study site. This difference can be explained by the difference in K_{matrix} between the two cases, which is clearly shown in Figure 5a. The K_{matrix} in the Rasse *et al.* (2000) study was high (3.2×10^{-6} m/s), while in the Bw and Bt horizons of this study, the K_{matrix} is 5×10^{-9} m/s. With root-macropore modification considered, the permeability contrast is located between Bt and CB horizons, or at a depth of 70 cm. This explains the observed vertical distribution of soil moisture, and supports Newman *et al.*'s. (2004) interpretation and the first two hypotheses of Wilcox *et al.* (1997), because the

CB horizon and the base of the Bt horizon play the same role provided that root macropores are absent at these depths. Since the existence of the third potential impeding layer at the soil-bedrock interface, located at the 100-cm depth, was not supported by the vertical soil moisture distribution (Figure 7), it was not further examined here.

To further test whether the absence of root macropores was the cause for low percolation into the highly permeable bedrock, two additional simulations with a modified CB horizon were conducted. In the first simulation, the CB horizon was replaced with tuff, leading to a 70-cm thick soil with root macropores in direct contact with the underlying tuff and resulting in significantly enhanced percolation (108 mm, Table II, column #5). In the second simulation, the CB horizon was replaced with a Bt horizon that included root macropores, resulting in a similarly enhanced percolation (105 mm, not shown). Optionally, we could add root macropores to the CB horizon. As the matrix hydraulic conductivity of the Bt and CB horizons is similar, the resulted annual percolation would be similar to the second simulation. Simulated percolation, when the root zone is in direct contact with the tuff, increases to approximately 20% of annual precipitation. This suggests that the low-permeability soil that lacks vegetation roots behaves as an impeding layer. It prevents significant percolation into the bedrock. If the ponderosa hillslope had a thinner soil cover, with the root zone in direct contact with the underlying permeable bedrock, the potential distributed recharge (percolation) could be as large as 20% of annual precipitation. This result indicates that the diffuse recharge at this environment, and other similar environments with low-permeability soil overlying permeable bedrock, can be highly variable, depending on the combination of soil thickness and root distribution.

CONCLUSIONS

Vegetation impacts soil moisture partitioning by two processes: root-water-uptake and root-induced macropore flow. The apertures surrounding vegetation roots can behave as macropores, or serve as preferential flow paths. An equivalent-continuum model is presented to quantify the root-induced macropore effect. The model-calculated root-macropore enhancement factors are consistent with the observations at the semiarid ponderosa pine site of this study, and at the alfalfa site reported by Rasse *et al.* (2000). The results indicate that the root macropore effect dominates saturated soil water flow in low permeable soils (K_{matrix} below 10^{-7} m/s), while it becomes insignificant in soils with K_{matrix} larger than 10^{-5} m/s.

At the ponderosa pine site, the model with simple root-macropore parameterization reasonably well reproduces soil moisture distribution and some major runoff events. The results indicate that the clay-rich soil layer without root-induced macropores behaves as an impeding layer for potential groundwater recharge. This impeding layer results in a bedrock percolation of less than 1% of

the annual precipitation. Without this impeding layer, percolation into the underlying permeable bedrock can be as much as 20% of annual precipitation. These results support the first two potential impeding layers hypothesized by Wilcox *et al.* (1997), as well as the interpretation for little deep percolation at this site by Newman *et al.* (2004).

ACKNOWLEDGEMENT

This work was primarily supported by the SAHRA (Sustainability of semi-Arid Hydrology and Riparian Areas) under the STC Program of the National Science Foundation, Agreement EAR-9876800, and partially supported by Flinders University Establishment Funding.

REFERENCES

- Allen RG, Pereira LS, Raes D, Smith M. 1998. Crop evapotranspiration—Guidelines for computing crop water requirements. Food and Agriculture Organization of the United Nations Irrigation and Drainage Paper 56.
- Altman SJ, Arnold BW, Barnard RW, Barr GW, Ho CK, McKenna SA, Eaton RR. 1996. *Flow Calculations for Yucca Mountain Groundwater Travel Time (GWTT-95)*. Sandia National Laboratory: Albuquerque.
- Beven K, Germann P. 1982. Macropores and water flow in soils. *Water Resources Research* **18**(5): 1311–1325.
- Brandes D, Wilcox BP. 2000. Evapotranspiration and soil moisture dynamics on a semiarid ponderosa pine hillslope. *Journal of the American Water Resources Association* **36**(5): 965–974.
- Carlier JP, Kao C, Ginzburg I. 2007. Field-scale modeling of subsurface tile-drained soils using an equivalent-medium approach. *Journal of Hydrology* **341**(1–2): 105–115.
- Dong WQ, Yu ZB, Weber D. 2003. Simulations on soil water variation in arid regions. *Journal of Hydrology* **275**(3–4): 162–181.
- Flint AL, Flint LE, Hevesi JA, Blainey JM. 2004. Fundamental concepts of recharge in the Desert Southwest: a regional modeling perspective. In *Groundwater Recharge in a Desert Environment: The Southwestern United States, Water Science and Applications Series*, Hogan JF, Phillips FM, Scanlon BR (eds). American Geophysical Union: Washington, DC; 159–184.
- Gee GW, Wierenga PJ, Andraski BJ, Young MH, Fayer MJ, Rockhold ML. 1994. Variations in water-balance and recharge potential at 3 Western Desert Sites. *Soil Science Society of America Journal* **58**(1): 63–72.
- Izbicki JA, Radyk J, Michel RL. 2000. Water movement through st thick unsaturated zone underlying an intermittent stream in the western Mojave Desert, southern California, USA. *Journal of Hydrology* **238**(3–4): 194–217.
- Mualem Y. 1976. New model for predicting hydraulic conductivity of unsaturated porous-media. *Water Resources Research* **12**(3): 513–522.
- Newman BD, Campbell AR, Wilcox BP. 1998. Lateral subsurface flow pathways in a semiarid ponderosa pine hillslope. *Water Resources Research* **34**(12): 3485–3496.
- Newman BD, Wilcox BP, Archer SR, Breshears DD, Dahm CN, Duffy CJ, McDowell NG, Phillips FM, Scanlon BR, Vivoni ER. 2006. Ecohydrology of water-limited environments: a scientific vision. *Water Resources Research* **42**(6): 15.
- Newman BD, Wilcox BP, Graham RC. 2004. Snowmelt-driven macropore flow and soil saturation in a semiarid forest. *Hydrological Processes* **18**(5): 1035–1042.
- Noguchi S, Tsuboyama Y, Sidle RC, Hosoda I. 1999. Morphological characteristics of macropores and the distribution of preferential flow pathways in a forested slope segment. *Soil Science Society of America Journal* **63**(5): 1413–1423.
- Phillips FM. 1994. Environmental tracers for water movement in desert soils of the American southwest. *Soil Science Society of America Journal* **58**(1): 15–24.
- Pneuli D, Gutfinger C. 1992. *Fluid Mechanics*. Cambridge University Press: Cambridge, United Kingdom; 496.
- Rassam D, Simunek J, van Genuchten MT. 2003. *Modelling Variably Saturated Flow with HYDRUS-2D*. ND Consult, Brisbane, Australia.

- Rasse DP, Smucker AJM, Santos D. 2000. Alfalfa root and shoot mulching effects on soil hydraulic properties and aggregation. *Soil Science Society of America Journal* **64**(2): 725–731.
- Renard P, deMarsily G. 1997. Calculating equivalent permeability: a review. *Advances in Water Resources* **20**(5–6): 253–278.
- Scanlon BR, Levitt DG, Reedy RC, Keese KE, Sully MJ. 2005. Ecological controls on water-cycle response to climate variability in deserts. *Proceedings of the National Academy of Sciences of the United States of America* **102**(17): 6033–6038.
- Simunek J, Jarvis NJ, van Genuchten MT, Gardenas A. 2003. Review and comparison of models for describing non-equilibrium and preferential flow and transport in the vadose zone. *Journal of Hydrology* **272**: 14–35.
- Stothoff SA, Or D, Groeneveld DP, Jones SB. 1999. The effect of vegetation on infiltration in shallow soils underlain by fissured bedrock. *Journal of Hydrology* **218**(3–4): 169–190.
- Stout DL, Sala A. 2003. Xylem vulnerability to cavitation in *Pseudotsuga menziesii* and *Pinus ponderosa* from contrasting habitats. *Tree Physiology* **23**(1): 43–50.
- Tromp-van Meerveld HJ, Peters NE, McDonnell JJ. 2007. Effect of bedrock permeability on subsurface stormflow and the water balance of a trenched hillslope at the Panola Mountain Research Watershed, Georgia, USA. *Hydrological Processes* **21**(6): 750–769.
- van Genuchten MT. 1980. A closed-form equation for predicting the hydraulic conductivity of unsaturated soils. *Soil Science Society of America Journal* **44**(5): 892–898.
- van Genuchten MT. 1987. *A Numerical Model for Water and Solute Movement in and Below the Root Zone*. U.S. Salinity laboratory: Riverside, CA.
- Walvoord MA, Phillips FM. 2004. Identifying areas of basin-floor recharge in the Trans-Pecos region and the link to vegetation. *Journal of Hydrology* **292**(1–4): 59–74.
- Walvoord MA, Plummer MA, Phillips FM, Wolfsberg AV. 2002. Deep arid system hydrodynamics—1. Equilibrium states and response times in thick desert vadose zones. *Water Resources Research* **38**(12): 1308, DOI: 10.1029/2001wr000824.
- Wigmosta MS, Vail LW, Lettenmaier DP. 1994. A distributed hydrology-vegetation model for complex terrain. *Water Resources Research* **30**(6): 1665–1679.
- Wilcox BP, Newman BD, Brandes D, Davenport DW, Reid K. 1997. Runoff from a semiarid ponderosa pine hillslope in New Mexico. *Water Resources Research* **33**(10): 2301–2314.